

## Simulation of Pore Formation in Lipid Bilayers by Mechanical Stress and Electric Fields

D. Peter Tieleman,<sup>\*,†</sup> Hari Leontiadou,<sup>‡</sup> Alan E. Mark,<sup>‡</sup> and Siewert-Jan Marrink<sup>\*,‡</sup>

*Department of Biological Sciences, University of Calgary, Alberta, Canada T2N 1N4, and  
Department of Biophysical Chemistry, University of Groningen, Nijenborgh 4, 9747 AG Groningen,  
The Netherlands*

Received November 27, 2002; E-mail: tieleman@ucalgary.ca; marrink@chem.rug.nl

Molecular dynamics simulations of pore formation and membrane rupture in phospholipid bilayers under mechanical and electrical stress at an atomic level are presented. Pore formation can be induced on a nanosecond time scale in simulations where the lateral pressure exceeds  $-200$  bar or where an electric field of  $0.5$  V/nm is applied across the membrane.

Lipid bilayer membranes are remarkable structures consisting of two leaflets of phospholipids. Their mechanical properties are central to understanding the behavior of cell membranes. For example, the formation of transient water pores is believed to underlie the passive transport of protons and hydrophilic compounds through the bilayer. Pore formation is also relevant during processes such as cell fusion and is important for drug release from liposomes. Experimentally, pores can be induced in membranes by applying mechanical stress (i.e., pipet aspiration experiments) or an electric field (electroporation). The precise mechanism by which pores form and their size, structure, and stability are, however, poorly understood.<sup>1–3</sup>

In previous simulation studies, pore formation has been observed in water/octane systems<sup>4</sup> and as an intermediate in the self-aggregation of phospholipids into bilayers.<sup>5</sup> Membrane rupture has been observed in simulations of simplified membrane models.<sup>6</sup> Here we present simulations of dipalmitoyl-phosphatidylcholine (DPPC) and dioleoylphosphatidyl-choline (DOPC) bilayers using a realistic force field in which the formation of water-filled pores is followed at atomic resolution.

Mechanical stress was applied as anisotropic pressure to a DPPC bilayer consisting of 128 lipids and 6029 water molecules, at a temperature of 323K with a 1.5 nm Coulomb cutoff. Simulations used the OPLS-based force field of Berger et al., the same as used in many previous studies.<sup>7,8</sup> A series of simulations (up to 50 ns) were performed. The lateral pressure was systematically varied from  $-50$  to  $-1000$  bar. The perpendicular pressure was held constant at 1 bar. A bilayer of 256 DOPC lipids and 11 228 waters (10–20 ns per simulation) was simulated with applied fields of 0.33, 0.4, and 0.5 V/nm at a temperature of 300 K and zero surface tension, with a 1 nm Coulomb cutoff plus Particle-Mesh-Ewald for long-range interactions.<sup>9</sup> Extensive simulations of DOPC and DPPC show that they behave essentially the same for the present purposes. All simulations were performed using the GROMACS set of programs.<sup>10</sup>

Figure 1 shows the time evolution of pore formation by mechanical stress. The equilibrated starting structure has an area of ca.  $0.6$  nm<sup>2</sup> per lipid. After stress is applied, this area rapidly increases, and pore formation began within 4–12 ns in three independent simulations. Once an initial rupture occurs, it grows rapidly, forming an approximately cylindrical pore that becomes lined with phospholipid headgroups. Water inside the pore is not

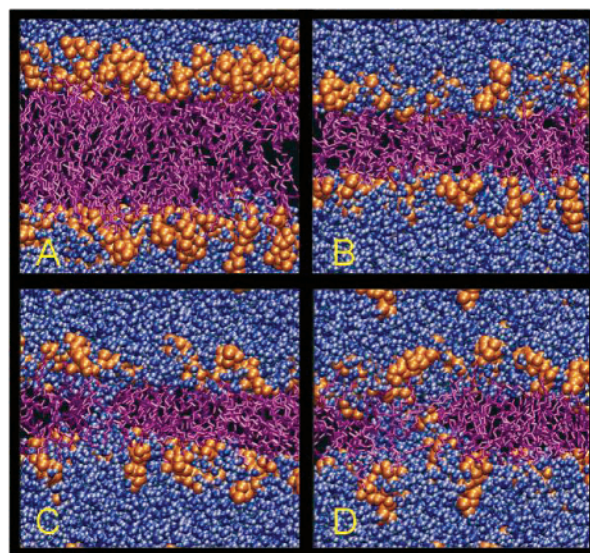


**Figure 1.** Pore formation by mechanical stress in DPPC bilayers (lateral pressure  $-200$  bar, ca.  $90$  mN m<sup>-1</sup>): (A) starting structure; (B)  $\sim 11.5$  ns, thinned bilayer after initial relaxation. Stages in pore formation and eventual rupture: (C)  $\sim 12.5$  ns; (D)  $\sim 12.6$  ns. Water is shown in blue, lipid chains in purple, and lipid headgroups in orange. All figures were made with VMD.<sup>11</sup>

oriented significantly. Once formed, the pore continues to increase in size until the bilayer is destabilized. Figure 2 illustrates the process of pore formation by an electric field. After the electric field is applied, there is a marked increase in defects where water penetrates into the acyl chain core. At a field of  $0.5$  V/nm, a pore forms rapidly (within 4 ns). The initial step in pore formation under both mechanical stress and an applied electric field appears to be the creation of a “single file defect” where a chain of water molecules spans the membrane. Such defects grow in size and become lined with phospholipid headgroups.

In pipet aspiration studies, the tension at which rupture occurs depends strongly on the rate at which it is applied, the loading rate.<sup>11</sup> At low rates the expansion of the pore is rate-limiting, and at high rates the formation of the pore itself is rate-limiting. At low loading rates, lipids expand only a few percent before rupturing at between 1 and 10 mN m<sup>-1</sup>.<sup>12</sup> At high loading rates, rupture occurs at progressively higher tensions immediately after pore formation. This is what is seen in the simulations where the effective loading rate is very high, and significant thinning is observed before pore formation due to the high tension. At low tension ( $9$  mN m<sup>-1</sup>), the percentage expansion of the membrane in the simulations is comparable to that experimentally observed ( $\sim 1$ – $2\%$ ).<sup>13</sup> Pore formation and membrane rupture is not observed on the time scale accessible. Once formed, however, pores are stable at a tension of up to 35 mN m<sup>-1</sup> (Leontiadou et al., manuscript in preparation).

<sup>†</sup> University of Calgary.

<sup>‡</sup> University of Groningen.

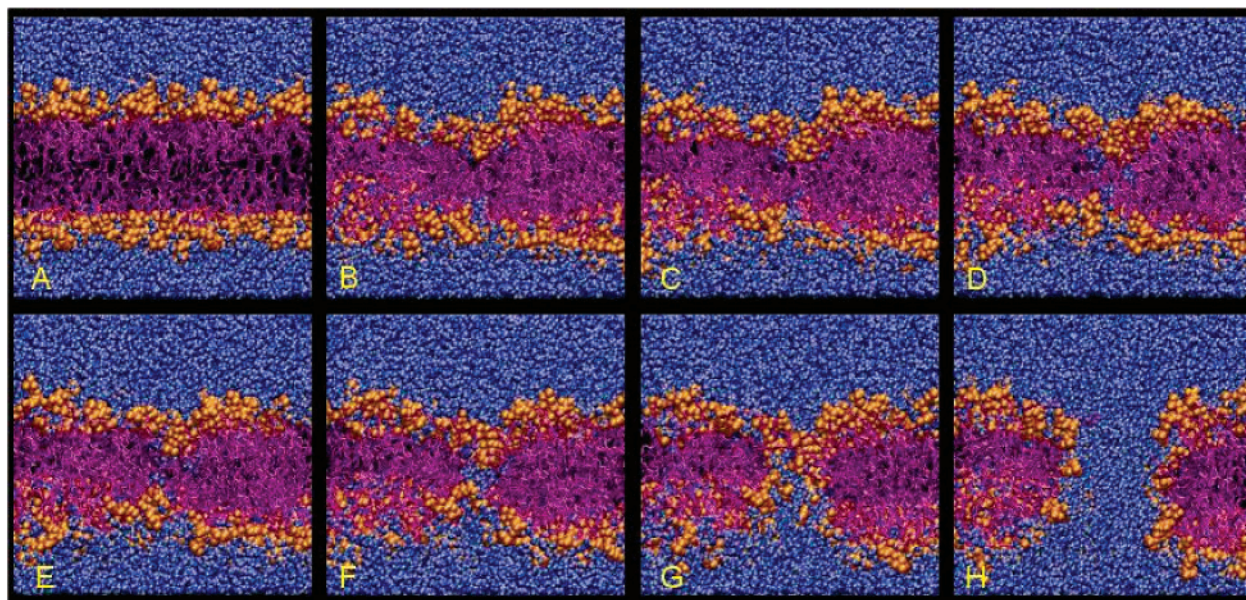


**Figure 2.** Pore formation in the DOPC simulation with an applied electric field of 0.5 V/nm: (A) structure at  $\sim 2.40$  ns, no obvious defects; (B)  $\sim 3.04$  ns, water penetration from both sides and significant deformation of the bilayer; (C–E)  $\sim 3.08$  to  $\sim 3.15$  ns, two defects from opposite sides of the bilayer form a single file across the bilayer; (F)  $\sim 3.25$  ns and (G)  $\sim 3.35$  ns, further rearrangement of the phospholipids and increasing size of the water column; (H)  $\sim 3.55$  ns, final size of the defect and nearly complete rearrangement of the phospholipids.

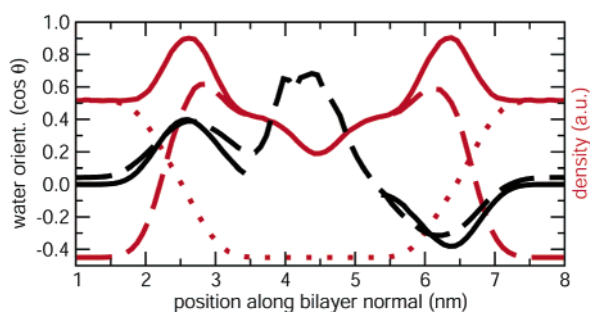


**Figure 3.** Water orientation along the bilayer with (black dashed line) and without external field (0.4 V/nm, black solid line). Without external field, water does not penetrate into the bilayer (gap). Also shown are the atom distribution of water (red dotted), lipid (red dashed), and all atoms (red solid) for orientation purposes. The center of the bilayer is at 4.5 nm.

The mechanism by which an applied electric field induces pore formation is uncertain. The field does interact with the charges within the headgroup. However, these interactions do not appear to be essential for electric-field-induced pore formation, which has also been observed in 3-nm-thick slabs of octane, which is uncharged.<sup>4</sup> Water is aligned by the field (Figure 3), but the effect near lipid headgroups is modest. Water penetration (before pore formation) increases significantly, and once inside the bilayer, water is strongly aligned by the external field (3.5–4.5 nm in Figure 3). Headgroup orientation is affected too: at 0.4 V/nm, before pore formation, the average angle between the P–N atom vector and the bilayer normal changes from  $12^\circ$  to  $8^\circ$  on one side, and to  $15^\circ$  on the other side of the bilayer, in both cases aligning the headgroup dipole with the external field.

At ca. 0.5 V, the potential difference used in the simulation is comparable to that used in black lipid membrane experiments, ca. 1 V.<sup>12</sup> Preliminary work suggests that pore formation can also be simulated at somewhat lower field strengths. One hypothesis that might explain the induction of pores is that the electric field stabilizes water defects, because isolated water molecules, or water molecules in small clusters, interact more favorably with the applied field inside the low-dielectric environment of the membrane than

in bulk water. In agreement with a recent continuum theory,<sup>2</sup> pores form with little change in area.

To summarize, the behavior of lipids and water within the bilayers differs, depending on whether a pore is induced by an electric field or by mechanical stress. In the presence of an electric field, water becomes highly oriented. Pores form with little change in surface area. In contrast, mechanical stress leads to significant thinning, at least at the high loading rates used in the simulations. In both cases, pore formation starts with “single file defects”, chains of water molecules that penetrate the bilayer from both sides of the membrane. Once two files touch, forming a full file, the chain of waters rapidly thickens, adopting an hourglass-like shape. This process is stabilized by the lipid headgroups simultaneously moving inward and lining the pore. Further simulations to investigate the lifetime and structure of pores, and the exact mechanism by which they form, are ongoing.

**Acknowledgment.** D.P.T. is an AHFMR Scholar and supported by NSERC. S.J.M. is funded by the Dutch Royal Academy of Sciences (KNAW). D.P.T. thanks Drs. J. Teissie and M. Winterhalter for their comments.

## References

- (1) Melikov, K. C.; Frolov, V. A.; Shcherbakov, A.; Samsonov, A. V.; Chizmadzhev, Y. A.; Chernomordik, L. V. *Biophys. J.* **2001**, *80*, 1829–1836.
- (2) Partenskii, M. B.; Dorman, V. L.; Jordan, P. C. *J. Chem. Phys.* **1998**, *109*, 10361–10371.
- (3) Wilhelm, C.; Winterhalter, M.; Zimmermann, U.; Benz, R. *Biophys. J.* **1993**, *64*, 121–128.
- (4) Tieleman, D. P.; Berendsen, H. J.; Sansom, M. S. *Biophys. J.* **2001**, *80*, 331–346.
- (5) Marrink, S. J.; Lindahl, E.; Edholm, O.; Mark, A. E. *J. Am. Chem. Soc.* **2001**, *123*, 8638–8639.
- (6) Groot, R. D.; Rabone, K. L. *Biophys. J.* **2001**, *81*, 725–736.
- (7) Berger, O.; Edholm, O.; Jahnig, F. *Biophys. J.* **1997**, *72*, 2002–2013.
- (8) Lindahl, E.; Edholm, O. *Biophys. J.* **2000**, *79*, 426–433.
- (9) Essmann, U.; Perera, L.; Berkowitz, M. L.; Darden, T.; Lee, H.; Pedersen, L. G. *J. Chem. Phys.* **1995**, *103*, 8577–8593.
- (10) Lindahl, E.; Hess, B.; van der Spoel, D. *J. Mol. Model.* **2001**, *7*, 306–317.
- (11) Humphrey, W.; Dalke, A.; Schulten, K. *J. Mol. Graphics* **1996**, *14*, 33–38.
- (12) Evans, E.; Heinrich, V. *Compte Rendus* **2002**, in press.
- (13) Winterhalter, M. *Curr. Opin. Colloid Interface Sci.* **2000**, *5*, 250–255.

JA029504I